Answer to reviewer 3

This is a very interesting analysis of a uniquely dense sea ice deployment of seismographs using ambient noise guided mode dispersion curves to invert for bulk ice properties (in two propagation directions). With a bit more detail (suggestions below) it's suitable for publication in its present form as an initial analysis of a data set that I strongly suspect has a lot more to offer in more detailed analysis. Will the data be publicly available somewhere (not apparently in the Acknowledgments).

Most of my comments below address where I suggest that methodological and other points might be usefully expanded (including, perhaps, some supplemental figures that could be in a appendix).

We thank reviewer for the positive feedback and all the suggestions and comments to improve the manuscript. Our answers are given thereafter. In accounting for the comments of the reviewers, we have added a figure in section 2.2.2 to describe the workflow for recovering the noise correlation function. We also added two figures in Appendix A to show the characteristics of the recorded seismic noise, and a figure in Appendix B to show the covariance of sea ice parameters.

The authors have done a good job in fitting analytical expressions to (beamform-selected) autocorrelations, with modes decomposed via a SVD method, to extract dispersion curves in EW and NS directions. The size and density of the array used (247 seismographs with interstation spacings as close as 1 m) is unprecedented to my knowledge for this type of application. Additional deployment and experimental details would be appreciated. Were the instruments buried, for example? Were ice cores taken for ice-truth measurements during of the experiment? How long did it take to deploy these instruments at this scale (important to know if such experiments might be repeated in other locations).

Reviewer 2 also requested more practical information about the deployments. Most of these details are available in Moreau, Boué, et al. (2019). However, we have added the following text to make the manuscript more self-consistent.

"The type of geophones used for the experiment has a cylindrical geometry of about 17 cm in height and 12 cm in diameter, mounted on a detachable spike. The geophones were installed directly in the ice without their spike. For accurate positioning, we used taut cords that we attached to each end of the rows and columns of the array, and a decameter. To maximize the coupling, a milling tool was specifically designed to drill the ice at the diameter of the nodes. The snow was removed prior to drilling holes, and geophones were installed in the holes at about half their height. We covered them back with snow to insulate them in view of preserving their battery life. At the time of the deployment, the internal temperature of several nodes was measured, before and after covering them with snow, showing an increase from -21 to -16°C. Deployment took about 2.5 days of work for a team of five people, including the time required for their activation. Markers were carefully placed all around the main array and at the position of the four antennae, in order to find them back more easily at the end of the experiment."

Could similar (or at least practically useful) results be obtained with a smaller deployment (this can be tested by decimating the data set of NCFs). This would be valuable to address given the motivations expressed in the abstract and paper.

This is an important point. We have demonstrated in Moreau, Weiss et al. (2019) that results with the same accuracy can be obtained by exploiting the waveforms of the icequakes recorded with as few as 3-5 stations. The methodology differs significantly from that in this manuscript, since it does not require to calculate the dispersion curves of the guided modes. A systematic inversion of the thousands of icequakes recorded during deployment will provide much more information about the spatial variations of sea ice parameters, that will not be limited to lines NS and EW. However, this requires to extract all the icequakes from the recordings.

This is an on-going work where deep learning strategies are being implemented to this end. Here we share some exciting upcoming results (see figure below), where part of these icequakes have been extracted and inverted for the source position as well as the ice thickness, using 5 stations only. Icequakes were recorded for the whole duration of the deployment.

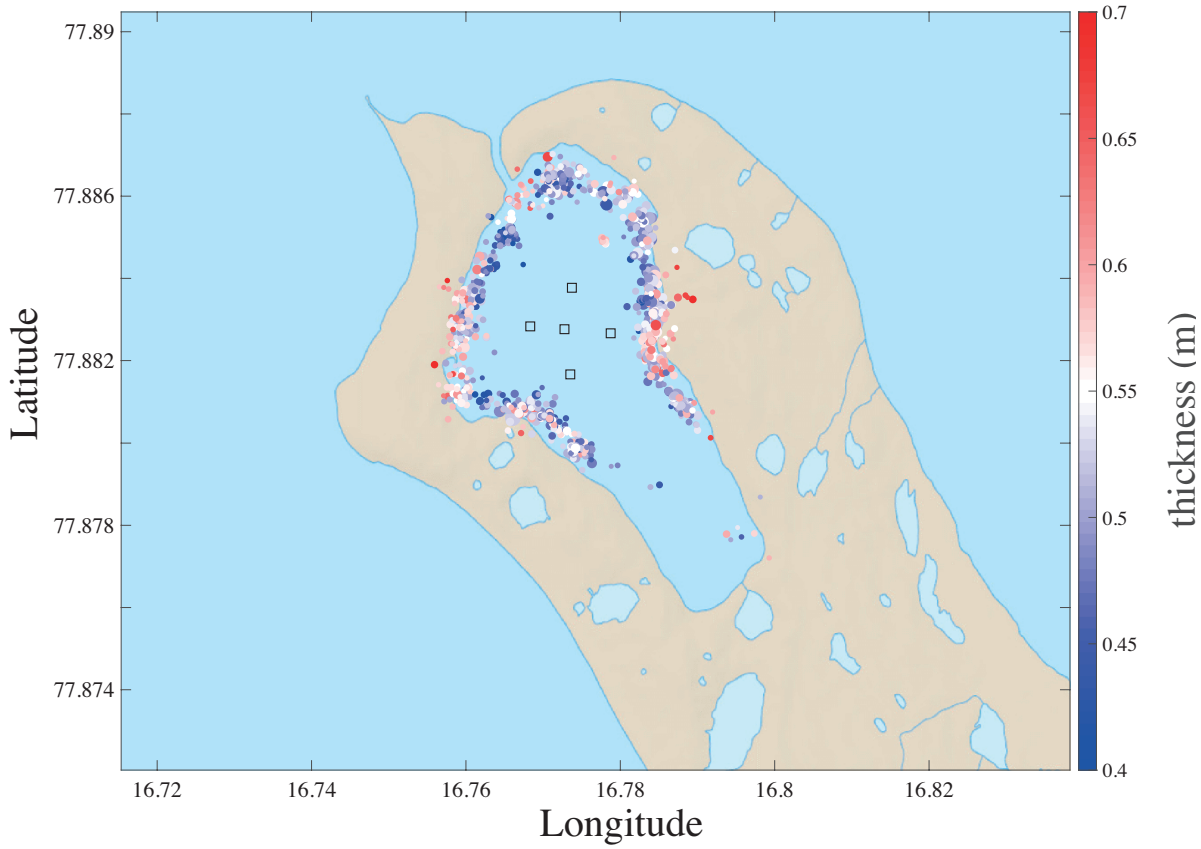

Icequakes (colored dots) extracted and inverted for source position and average ice thickness between source and the 5 stations used for inversion (shown as black squares). Icequakes were recorded between 27 February and 24 March 2019. Note the change in thickness for icequakes coming from the same position, which indicates that ice has grown during deployment. The inverted ice thicknesses are consistent with those found using the EW and NS array lines and the processing introduced in the present paper. The location of the icequakes follow the shore line, where cracks have been visually identified. These cracks were likely cause by thermal and tidal forcing.

Complicating methodological or physical factors that may explain the observed variance in the parameters were underexplored (e.g., can the dispersion curves be better resolved or meaningfully smoothed to improve the data as shown in example in Figure 4?).

Reviewer 1 also asked if it would be possible to improve the retrieval of the dispersion curves. We have elaborated on the SVD-based processing to explain why it is unlikely to obtain better results from currently available alternative strategies. This is essentially due to the fact that the SVD already accounts for the multiplicity of virtual sources (i.e. the four stations in each of the four linear arrays to the east, west, south and north) in an optimal way. We have added the following explanations.

This processing consists in the following steps:

1. The matrix of transmit-receive signals has three-dimensions: sources (M = 2 or 4), receivers (N), and time. The first step is the application of the Fourier transform to the temporal dimension of this matrix.

2. At each frequency, the resulting Fourier-domain matrix is sliced into 2D transmit-receive matrices. These matrices are then decomposed into singular values. The singular vectors define an orthonormal basis of the space dimensions along the transmitters (left-singular vector) and receivers (right-singular vector). The underlying idea behind this processing step is that the different levels of modal energy are distributed onto the singular vectors, the energy information being contained in the singular values. This allows a heuristic separation of the noise and signal subspaces, in a classical way for singular value-based filters.

3. The last step consists of defining test vectors that are representative of the wave propagation problem. In the present case, we use plane waves of the form $e^{-ik_{test}x_n}$, where k_{test} is the

wavenumber to be tested, and x_n (n = 1,2,...,N) is the coordinate of receiver n along the propagation. Finally, the test vectors are projected onto the singular vectors of the receivers' basis. This leads to a scalar product that is maximized when the wavenumber in the test vector matches that of the waves in the measured wavefield. In practice, this projection step is equivalent to calculating the discrete spatial Fourier transform of each singular vector.
Step 3 is performed at each frequency resulting from step 1.

Once steps 1-3 are performed, the resulting frequency-wavenumber spectrum significantly enhances the identification of the dispersion curves, for two reasons: (i) it is possible to separate signal from noise by applying a threshold to the singular values; and (ii) modal amplitude stands out at all frequencies and for all modes with the same spectral intensity (Fig. 4), despite their different relative amplitude in the wavefield, because singular vectors have a unit norm. The dispersion curves can therefore be identified on a larger bandwidth and with less SNR-related uncertainties than with conventional beamforming techniques (Moreau, Boué et al, 2020).

It was unclear (to me) exactly which stations were being correlated for use in constraining the NCFs (e.g., the linear array stations and azimuthally selected stations in the grid (which would mean that only stations intersecting a 10-degree cone from the linear array stations were actually utilized, but no stations from the corners, for example (?)). It would seem that a great many potential cross-correlations within the experiment were not used. That's fine for this initial study, but some additional detail and quantification of this geometry and data usage would be appreciated (with 247 stations there are potentially around 30,000 potential NCFs that could be calculated, of course; how many total NCFs went into the inversions here out of these potential ~30,000 station pairs?). I'd suspect that a more comprehensive subarray strategy might yield improved results, and the ability to assess spatial variations (the authors hint that this will be a next step, along with icequake analysis in future work at the end of the paper). Structural variation across the study region may explain some of this four-parameter estimation experiment (but again it's not clear to me but it would be nice to assess this effect more thoroughly; it's alluded to for example in line 270).

The reviewer is right, and much more information about the ice could be obtained by using all station-pair combinations to calculate the correlations. We have added the following explanation to justify why we restrict the study to the stations of the dense cross and the linear arrays only.

In this work, we restrict the study to correlations between (i) the 45 stations of the EW line with the 4 stations of the LEA and LAW, and (ii) the 45 stations of the NS line with the 4 stations of the LAS and LAN. Of course, by using all stations pairs amongst the 248 stations, it will be possible to obtain 30381 inter-correlations with many different inter-station paths, distances, and directions. With such amount of correlations, it becomes possible to apply tomographic inversions over the full array geometry, and to obtain a 3D+time map of the sea ice properties with unprecedented spatial and temporal resolution. However, this requires a different processing strategy where noise sources have to be selected so that their distribution around the array is isotropic. This is an on-going work that will be the matter of a future paper.

The authors employ a simulated annealing strategy to obtain a starting model. It was unclear to me, at least, how this leads to new information regarding determination of the measurement errors, unless this was simply evaluated to be consistent with the chi-square value, which is simply consistent). For this reason. I suggest that it is more accurate to indicate that the fit (e.g., line 280) between model and data is statistically "consistent", rather than "excellent".

In a way, we are indeed attempting to be consistent with the chi-square value, so we have replaced "excellent fit" with "statistically consistent fit". Reviewer 2 also asked about the interest of the simulated annealing phase. Here we give the same answer.

We agree with the reviewer that this may look unclear. The problem when trying to estimate sigma comes from the fact that it should account for uncertainties in the dispersion curves, not those in the measurements. There is no linear relationship between both, because of the dispersion of the QS mode. That is what we had tried to explain in section 2.4.2 when writing:
"The variance is linked to measurement errors; i.e., a mix between the influence of the SNR and other random perturbations of the measure, such as variations in the physics of the problem. In the present problem, such perturbations are averaged when going from the time-space to the frequency-wavenumber

domains, and thus the variance reflects variations of frequency- wavenumber values around ground truth values."
Moreover, depending on the quality of the correlation function, these variations are not the same between all sets of dispersion curves. This is why we have chosen to estimate sigma from the simulated annealing part.
In an attempt to make this clearer in the manuscript, we have added the following explanations.

"However, σ^2 is data-dependent. In our approach, we are inverting dispersion curves, so it should account for uncertainties in the dispersion curves, not those in the measurements. Unfortunately, there is no linear relationship between both, because of the dispersion of the QS mode. Depending on the quality of the correlation function, these uncertainties are not the same between all sets of dispersion curves. Hence σ^2 cannot be set *a priori* for all of the inversions in this study, or else it would be a coarse approximation."

They subsequently use MCMC to obtain a posterior PDF with a uniform (limited) range prior distribution for each parameter, but do not show the covariances of the parameters. A posterior illustration of parameter covariances would also be helpful to illustrate the tradeoff space between the four parameters.

The range of prior distribution was chosen so as to include values found in literature for first year ice. We have added the following justification:

For first year ice, in situ measurements of density range from 840 to 910 kg/m3 for the ice above the waterline, and 900 to 940 kg/m3 for the ice below the waterline (Timco and Frederking, 1996). Poisson's ratio varies between 0.25 and 0.4, Young's modulus between 2 and 6 GPa (Anderson, 1958; Timco and Weeks, 2010). In particular, in the Van Mijen fjord, Romeyn et al. (2021) reported a Young's modulus around 2.5 GPa with a Poisson's ratio of 0.33, and Morozov et al (2012) reported a Young's modulus around 3 GPa and a Poisson's ratio of 0.3. (Moreau et al, 2014c), reported a Young's modulus around 4 GPa and a Poisson's ratio of 0.32 at Vallunden. The slightly higher value of Young's modulus at Vallunden, in comparison with those directly in the Van Mijen fjord, is likely attributable to the protected physical setting of the study site, and support from the surrounding shoreline at the moraine. Regarding the thickness, ice drillings indicated that it was systematically less than 1 m. Hence, we assume for the prior distributions that the model parameters have equal probability over a range of values that contains the above-referenced values.

We have added a new figure in Appendix B (see below), which shows the covariance between parameters. We have also modified the comments regarding the PDF accordingly:

Interestingly, the covariance of the parameters (see figure B1 in Appendix B) indicates that Poisson's ratio, despite being well-constrained, seems rather uncorrelated from the other parameters. On the other hand, Young's modulus, density and thickness appear to be strongly correlated, despite the density being not very well-constrained.
The observations seem to indicate that density having a flatter PDF reflects the limits of our forward model more than it is an indicator of the limits of the methodology. The model is only sensitive to the effective properties of the {ice+snow} system, because it cannot account for the snow layer (about 40 cm thick, on average), which modifies the effective properties. The weight of the snow layer modifies the density of the {ice+snow} system more than it does its rigidity (Young's modulus) and expansion/contraction (Poisson's ratio). Presumably, a forward model able to account for snow would be a significant improvement, which should constrain the density in a better way. The development of such a forward model is therefore an important follow up of this work.

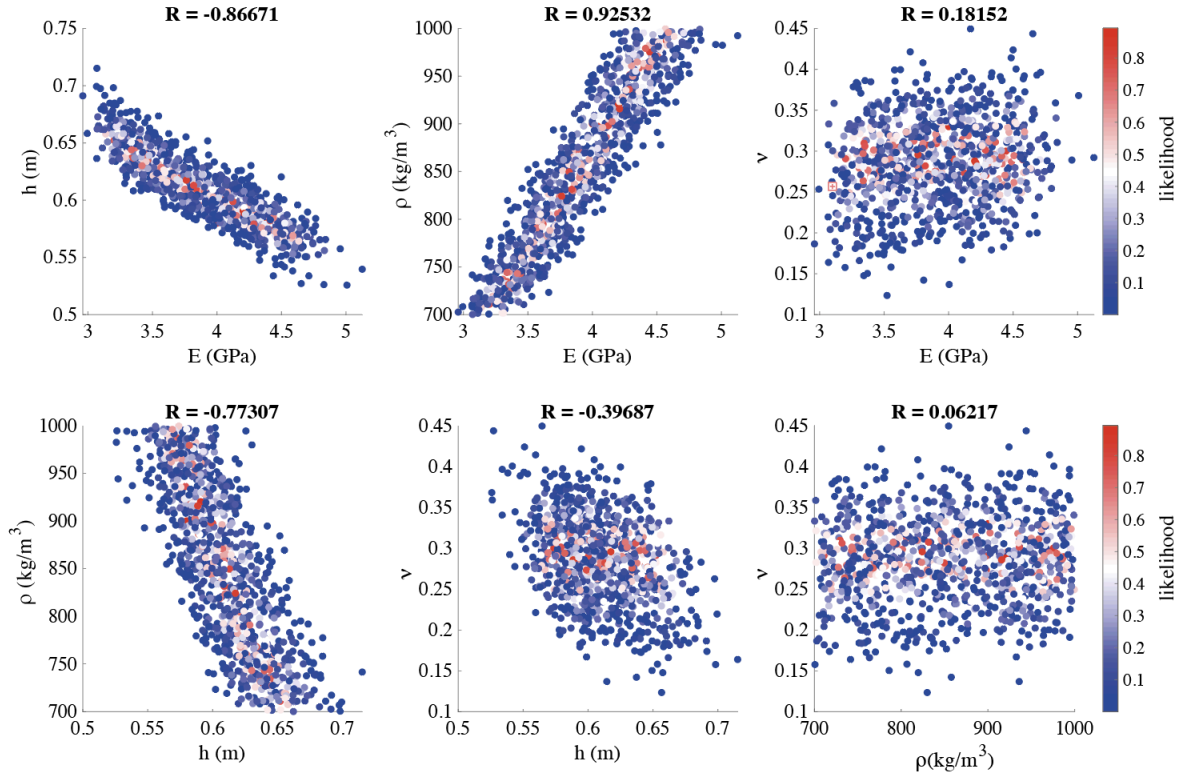

Figure B1. Covariance between Young's modulus, thickness, density and Poisson's ratio, with the associated correlation coefficient

It is interesting that the inferred ice thicknesses differ systematically in the NS and EW directions in Figure 7. Can the authors elaborate on this (in line 270 they allude to special variations in the physics of the problem, but I believe what they meant to indicate was something like "spatial variations in ice model parameters".

We meant "spatial variations" indeed. This has been modified. We do not have a clear explanation for this. A likely explanation could be related to the elongated geometry of the moraine in the NS direction, which could have a mechanical effect to the ice while it is growing. Also, the channel to the north, where water current is present could have an effect. However, it is noteworthy that the differences between both directions are not statistically significant, since the uncertainties overlap, so it could also be linked to the quality of the Green's function retrieval. This remark was added to the manuscript.

All things considered, this is a significant work with a unique data set that could use a bit more polishing to realize its potential, and will no doubt be valuable for further analysis.